1 Quantum Effects in Sub-nm Gaps between Spherical-Tipped AFM Probes

Should the surfaces of two approaching spherical surfaces be sufficiently clean that the formation of a sub-nm gap becomes possible, the influence of quantum effects on plasmonic coupling becomes readily observable. By monitoring the electrical conductivity simultaneously with the optical scattering the effects of quantum charge transfer on plasmon coupling can be directly inferred under the assumption that the d.c. conductance is similar to the conductance at optical frequencies. Using this approach, the quantum limitations to plasmonics can be observed in full for the first time. This section discusses the now readily attainable regime of plasmonics in sub-nm gaps. The investigation into the effects of quantum charge transport on plasmon coupling is the culmination of all previous developments to date, yielding some of the most interesting results of this project.

To briefly reiterate theory, according to [**zuloaga2009**], between separations of ∼0.3 nm and 1 nm gaps are expected to be in the crossover regime, where classical theory breaks down due to the onset of quantum tunnelling. Gaps are characterised by a thin barrier between particles with a growing probability for electrons incident on the barrier to tunnel through it. The non-locality of surface electrons smears gap surfaces on the quantum level, rounding the potential barrier in the gap once wavefunctions begin to overlap. Long-range interactions between image charges also function to round the barrier. Tunnelling-induced charge transfer neutralises charge on the gap surfaces and reduces electromagnetic coupling. This decreases, and eventually halts, the rate of redshift and is otherwise known as the screening effect. Beyond ∼0.3 nm the increasingly overlapping wavefunctions cause the potential barrier to drops below the Fermi level, creating a conductive constriction. Ballistic conduction now applies and gaps enter a quantised conductive regime. The increased currents cause hybridised modes to further decouple, blueshifting their resonances as they transform into CTPs.

These regime boundaries described by recent theory are often only a guideline as to what can be expected, with reported threshold separations for entering a conductive regime varying between 0.2 nm [**zuloaga2009**] and 0.3 nm [**esteban2012**, **savage2012**, **scholl2013**, **esteban2015**] (and in some predictions even larger separations [**barbry2015**]) depending on the specific dimer geometry and materials. Suggestions have also been made to indicate that current contributions from two cooperative conductive channels can sum to an effective conductance, meaning larger particles should enter the quantum regime at larger separations when compared with smaller particles of the same material. In previous measurements this critical gap size has been determined by either comparing to theory [**savage2012**], or by TEM measurement [**scholl2013**]. However, despite the frequent observation of a critical gap size of 0.3 nm, this quantity is by no means fundamental and is therefore not the most appropriate standard by which to compare experiments. For example, the addition of molecules in the gap, where the gap size is set by the length of the molecular spacer layer, results in an earlier onset of conductive regime characteristics [**tan2014**, **hajisalem2014**]. The critical separation is simply the point at which conductive charge transfer overpowers capacitive interaction, hence a set of critical conductances should exist for entry into each respective regime of quantum interaction, irrespective of gap size, that more fundamentally describe the effects of quantum transport on plasmon coupling.

As theory has previously suggested, critical conductances at optical frequencies are a more appropriate way of describing the regimes of quantum charge transfer behaviour [**perez2011**, **benz2014**]. Experimentally this proves incredibly difficult. In a sense, plasmonics is the only way of measuring an optical conductance. Electronic equipment cannot respond fast enough to measure currents at optical frequencies. One reason as to why charge transfer effects should be understood is therefore to enable the application of plasmonics as a method of measuring conductance at frequencies where standard electronic technologies fail. At this time however, the d.c. current through the gap is measured as an approximation to the electronic behaviour at optical frequencies to compare with the

effects seen in optical spectra. Using this, the current set of experiments explore the concept of critical conductances as the definitive way of interpreting charge transfer in plasmonic systems.

1.1 Observations of Quantum Charge Transport in Plasmonic Cavities

Figure 1 shows a selection of spherical Au tip dimer measurements showing both optical and electronic behaviour once in the sub-nm regime. Simultaneous quantum transport and SDF scattering measurements are presented as a function of the applied force on the gap. Each of the measurements exhibits the signatures of a transition between hybridised and charge transfer plasmons. Interestingly, each scan in the sub-nm regime manages to appear somewhat different in terms of mode behaviour, regardless of any similar agreement between scans in previous coupling regimes. These differences are thought to originate from surface roughness or even smaller differences in sub-nm scale morphology that affect the way optics and electronics couple. Correctly interpreting and understanding these results is of general importance within the current plasmonics community as smaller gaps begin to become experimentally attainable and the blending of plasmonics and molecular electronics becomes commonplace. To begin the discussion, each set of measurements is initially considered individually.

Both Figures 1a and 1b bear the closest resemblance to the original simulated QCM spectra of sub-nm gaps between spherical Au tips (replotted in Figure 1d with the DFT-calculated conductance density overlaid) [**savage2012**]. Each show the screening of hybridised plasmons and the emergence of CTPs. Screening is indicated by a reduction in the rate of redshift and a decrease in intensity, which is followed by a blueshift and the formation of CTP modes signifying the rise of stronger interparticle currents. In theory, these critical currents occur at a conductance density of $0.4\,\mathrm{G_0\,nm^{-2}}$, at which point two CTPs emerge and hybridised modes disappear. The transition from hybridised plasmons into CTPs is clearly observed in experimental data, with modes appearing at similar wavelengths. The fundamental CTP is not measurable using the current microscope as it is expected to exist in the IR, outside the wavelength range of the spectrometers. The neck of the tip may also act as a short for this mode, preventing it from appearing at all. The behaviour of hybridised modes and higher order CTPs is thus used to interpret the behaviour in the gap.

In both experimental cases, the redshift of each hybridised modes becomes stunted once the conductance rises above $\sim 10^{-3}\mathrm{G_0}$, indicating the onset of screening. This is the first critical conductance, revealing the point at which electron tunnelling has risen enough to effectively begin screening gap coupling. The point of blueshift is less clear in Figure 1a due to the fast transition into geometrical contact. This jump is experienced in almost all scans once the electrostatic pull of the tips is large enough to overcome the meniscus forces holding surfaces apart. Figure 1b provides a much clearer insight into the origins of the blueshift, and is likely the single most informative scan, demonstrating each of the quantum effects and showing good agreement with the principles underpinning recent theoretical models [**zuloaga2009**, **savage2012**]. Its tip approach is much more carefully controlled into geometrical contact, with many measurements in the tunnelling regime and clear observation of discretely quantised conductance channels. It is at this transition between tunnelling and one-dimensional conduction, at around $2\mathrm{G_0}$, that the blueshift begins to occur and tips enter the quantum conductive regime.

A better view of this transition is shown in Figure 2a where the scan shown in Figure 1b is replotted with a linear conductance scale in order to closer inspect charge transfer behaviour. The turning point in the redshift of both hybridised plasmons visually appears to be at $2\mathrm{G_0}$ in spectra. Fitting the spectra and extracting the behaviour of each individual mode provides a more quantitative analysis. The results of the fit are superimposed onto spectra in Figure 2a with relative peak shifts and mode parameters shown separately in Figure 2b. Mode positions follow an exponential model as expected. At $2 \times 10^{-3}\mathrm{G_0}$ the redshift deviates from this model and becomes less pronounced. Prior to this point the amplitude of the lower order mode is decreasing, likely due to increasing charge localisation. Upon passing through the first critical conductance at $2 \times 10^{-3}\mathrm{G_0}$ the amplitude is

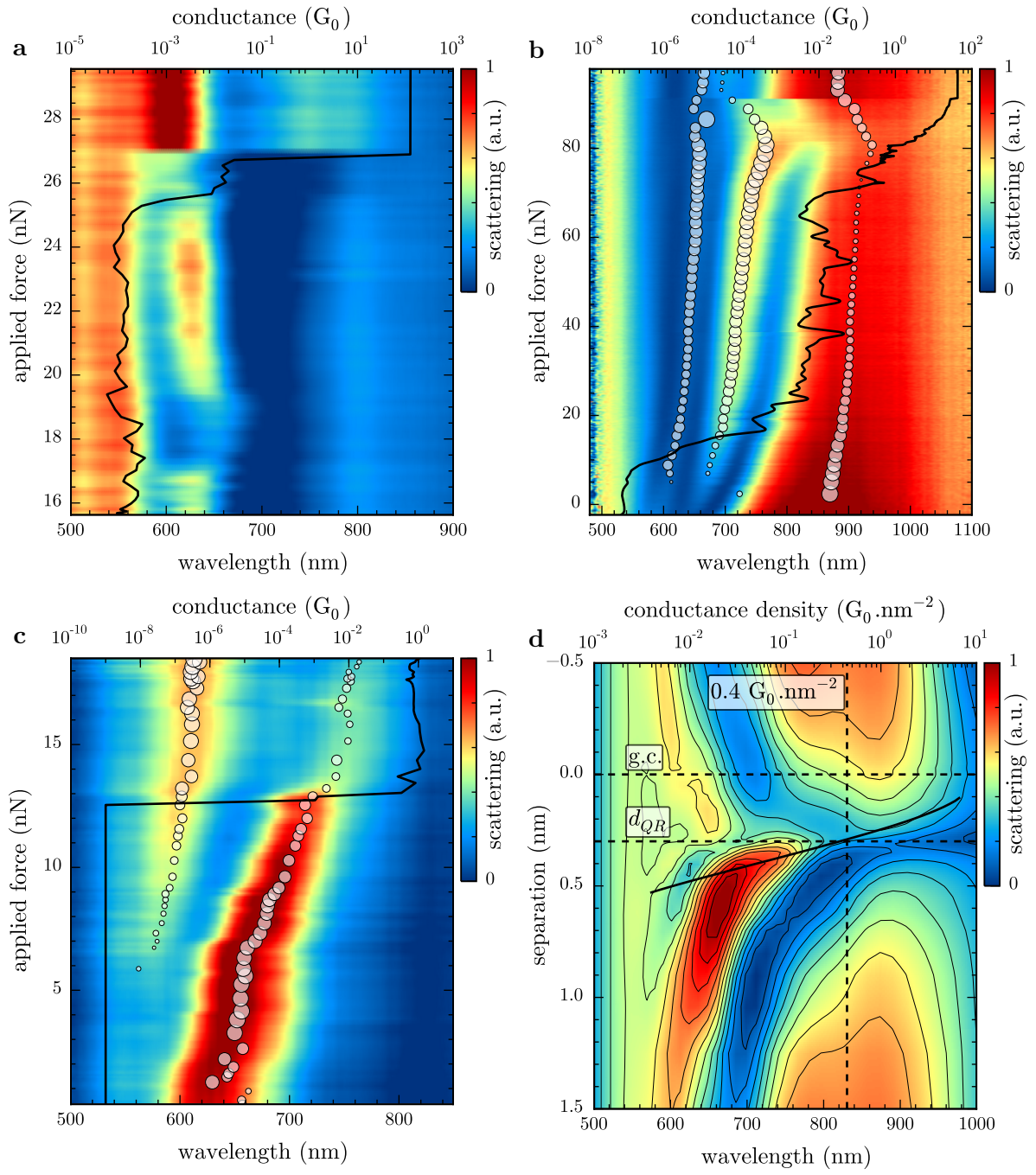

Figure 1: Scans of multiple spherical tip dimers passing through the quantum regime and pushing towards geometrical contact. Scans (a–c) show the supercontinuum dark-field scattering spectra as a function of the applied force on the gap with the simultaneously measured conductance superimposed over the axis. The circles highlight the position of the peak. The size of the circle indicates the amplitude of the mode in the fitted model. Scans (a) and (b) use Au-coated NanoTools B150 spherical AFM probes to form a dimer while scan (c) uses electrochemically-fabricated AuNP-on-Pt AFM tips. Calculated QCM spectra of a spherical tip dimer as a function of separation, replotted from [**savage2012**], is shown in (d). Simulated spectra show that both bonding modes disappear prior to geometrical contact (g.c.) at $d_{QR} = 0.3\,\mathrm{nm}$ and are shortly followed by the rise of CTP modes. This occurs since quantum electronic transport transfers enough charge within half an optical cycle to screen hybridised plasmons and eventually excite a CTP. Based on DFT calculations the CTP is excited when the conductance density is $0.4\,\mathrm{G_0\,nm^{-2}}$. These effects are seen in experimental scans once the conductance surpasses $2\mathrm{G_0}$.

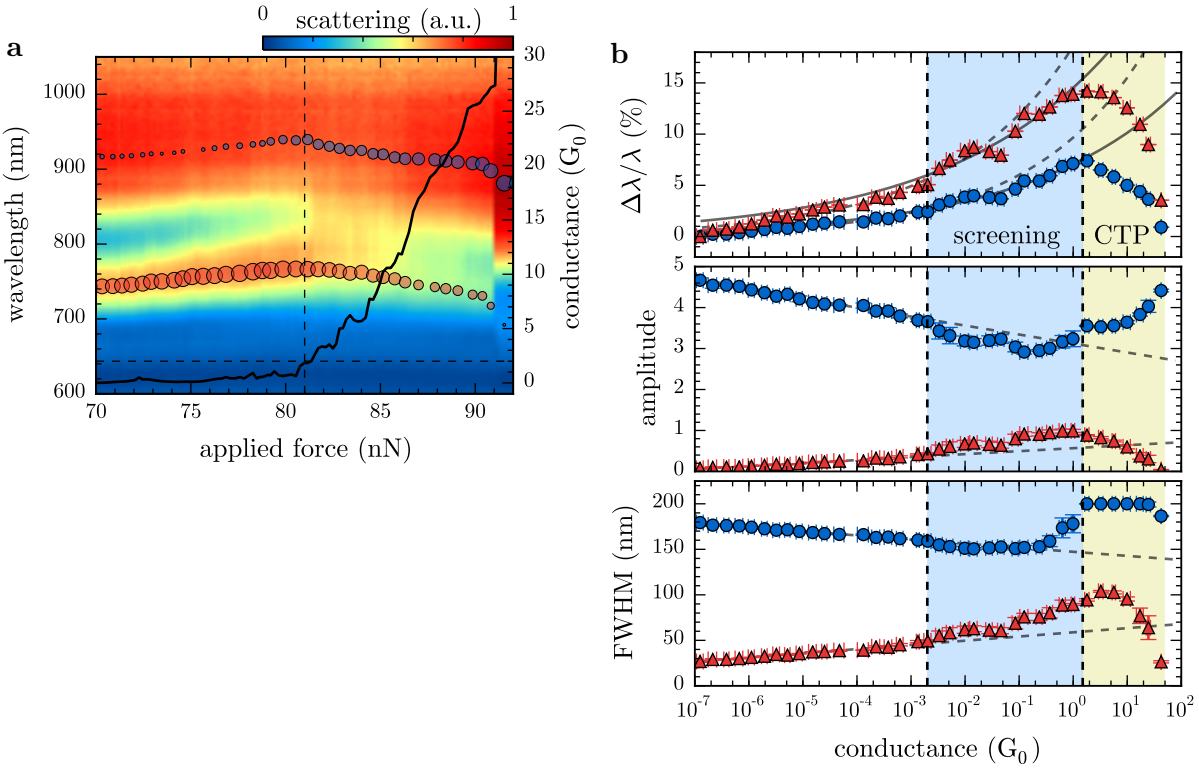

Figure 2: Detailed analysis of a spherical Au tip dimer scan in the quantum charge transfer regime. The scan shown in Figure 1b is replotted in (a) with a linear conductance scale to show quantised conductance stepping and its relationship with scattering spectra. Dashed lines indicate the point of blueshift at $G = 2\mathrm{G}_0$. Peak positions in the fitted model are denoted by circles superimposed onto spectra with their size corresponding to the peak amplitude. The relative shift of each mode from fitted parameters, along with a normalised amplitude and FWHM, are plotted in (b). Vertical dashed lines highlight the transitions into the tunnelling (crossover) regime at $2 \times 10^{-3}\mathrm{G}_0$ and the conductive regime at $1.5\mathrm{G}_0$. Exponential curves are fitted to the wavelength shift for $G < 10^{-3}\mathrm{G}_0$ (dashed) and $G > 2 \times 10^{-3}\mathrm{G}_0$ (solid) to highlight the reduction in redshift caused by passing through the screening (tunnelling) threshold. Similar lines are plotted to show changes in the amplitude and width upon passing through $2 \times 10^{-3}\mathrm{G}_0$.

further screened and decreases faster. The higher order mode continues to gain intensity at this point, potentially from redistributed charge of the lowest order mode. Similar behaviour is found in the mode widths.

The second critical conductance can be defined as $2\mathrm{G}_0$, a surprisingly appropriate quantity given that it occurs just above the transition from tunnelling into a quantum conductive regime. Upon surpassing $2\mathrm{G}_0$ the resonance position of both hybridised plasmons begins to strongly blueshift into CTPs as current passes through the junction, quickly returning to their initial resonance position prior to entering the tunnelling regime. During this transition the intensity and width of the lowest energy plasmon begins to increase, while the higher order plasmon attenuates into only a weak, blueshifted resonance. This CTP becomes fully developed during the final pull into geometrical contact. A third critical conductance for CTP development can then be estimated to be around $10\mathrm{G}_0$ with full development between 30–$40\mathrm{G}_0$.

Despite integer quantised conductance steps being observed in this conductive regime, there is no obvious step-wise behaviour in the optics. Given that it is the charge transfer that leads to the blueshift of hybridised modes it would be intuitive to expect quantised current changes to discretise incremental blueshifts. This is not obviously the case, with the blueshift appearing smooth throughout. More experimental data would be needed to properly understand this observation.

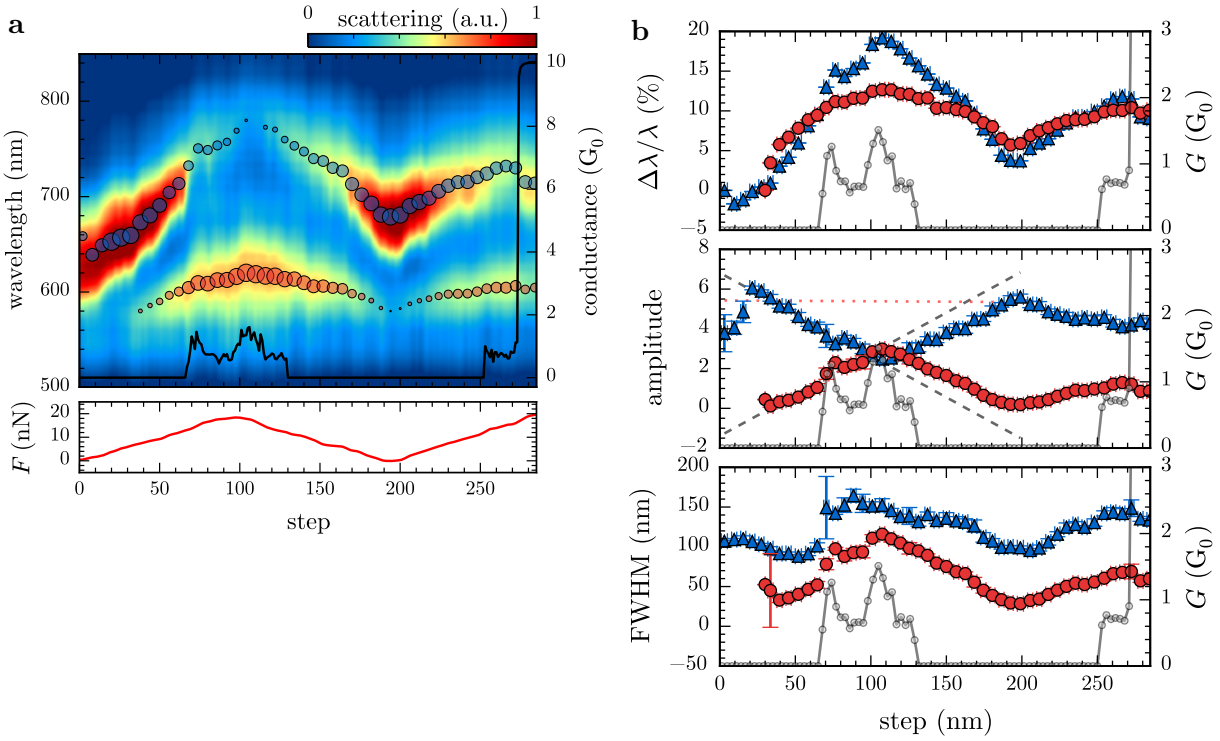

Figure 3: Detailed analysis of the extended electrochemically-fabricated spherical AuNP-on-Pt tip dimer scan. An extended plot of the scan shown in Figure 1c is plotted in (a), demonstrating reproducibility in approaches. The applied force trace represents the separation changes between tips, with tips approached, retracted and then finally approached into geometrical contact. Peak positions in the fitted model are denoted by circles superimposed onto spectra with their size corresponding to the peak amplitude. The relative shift of each mode from fitted parameters, along with a normalised amplitude and FWHM, are plotted in (b). Linear rates of amplitude variation are revealed from peak fits, removing the width contribution from the peak intensity. The FWHM of each mode increases with conductance. Reduced rates of redshift are found in the $G \sim 1\mathrm{G}_0$ regions with a discontinuous blueshift seen after the $G > 2\mathrm{G}_0$ transition.

Both sets of measurements at the focus of this discussion are not without their issues, however, when comparing with both theory and previous experimental results. Figure 1a shows variations in both the position and intensity of the 600 nm mode, which are attributed to changes in the torsional force on the gap, corresponding to a rotational motion of the tip. The mode also does not appear to shift as much as expected. The intensities of the final two modes when in contact are also reversed compared with QCM predictions. Figure 1b looks remarkably closer to theory. Changes in CTP position and intensity are said to originate from the touching profile of the dimer, indicating that the surface roughness may play a role with such large dimer surfaces [**zuloaga2009**, **barbry2015**].

Figure 1c shows a somewhat different phenomena to previous scans, though still in line with quantum transport expectations. Tips in Figure 1c are highly asymmetric AuNP-on-Pt tips, smoothed using piranha solution. Both have $40\,\mathrm{N\,m^{-1}}$ cantilever spring constants, hence the force resolution during approach is limited. Prior to tunnelling a higher order mode begins to emerge. The transition into contact is quick, with few to zero points at any given conductance, ending initially with a stable 0.75–$1.5\mathrm{G}_0$ contact. Once the conductance has risen the initial LSP resonance quickly diminishes without blueshifting and the higher order resonance gains intensity. The screening here is another example of entering into a tunnelling regime but without sufficient current to progress into the conductive regime and blueshift existing LSPs into CTPs.

After the initial conductance increase, the tip is then retracted to test for reproducibility, as shown

in the extended scan plot in Figure 3a. This is made possible by the robustness of electrochemically fabricated tips, with their solid AuNP apices. Attempting this with commercial, spherical Au tips results in the spherical tip separating from the neck due to adhesion forces. A second approach of the tip immediately after retracting out of contact demonstrates the same phenomenon until the conductance rises above $2G_0$ when both modes blueshift. Changes in the redshift and amplitude gradient show the effects of surface roughness as retraction introduces a small degree of misalignment between tips such that the point of closest contact in the second approach is different from the first.

A detailed mode analysis of the plasmon resonances is shown in Figure 3b, in which the trends described for previous measurements still apply. The peak position behaves as expected. Upon increasing the conductance up to the $1G_0$ level there is a visible kink in the redshift as its rate reduces as a result of screening. Once the conductance rises above $2G_0$ in the second approach there is a clear blueshift in the lowest order mode. This is a similar, although more abrupt, measurement of the critical conductance than in previous scans. The amplitude behaviour extracted from peak fits is interesting in this case since the amplitude of the initial mode linearly decreases during approach at exactly the same rate of increase as the emerging mode. This equality in the gradients is shown by the dotted red line in the figure indicating the constant sum of the two amplitudes. In a sense, charge is conserved and simply switches to a more favourable mode as the gap width decreases. Conceptually, this could suggest that tunnelling begins to reduce coupling between the lowest order modes first, making higher order coupled modes energetically more favourable.

Each of the presented three scans show agreement with recent theoretical concepts that define the influence of quantum transport on plasmon coupling. Critical conductances for entering the tunnelling regime and the quantum conductive regime are observed in each case in the vicinity of $1\text{–}2 \times 10^{-3}G_0$ and $2G_0$, respectively. No observation of the fundamental CTP excitation has been made leaving the final critical conductance yet to be experimentally measured. This is the first time conductance values have been correlated dynamically with optical spectra. Comparison with previously explored systems shows excellent agreement, supporting the idea of a set of fixed critical conductances. Blueshifts of the BDP, forming the SBDP, begin to be seen in small conductive contacts at conductances of $2G_0$ in both theoretical models [**perez2010**, **perez2011**] and experimentally in the NPoM geometry when AuNPs are separated from a Au mirror by a blended SAM of variable conductance [**benz2014**]. Observation of the same threshold conductance in two very different systems provides strong evidence for the fundamental nature of critical conductances. Variations in measured quantum transport phenomena between tip dimers are highly likely to be the result of surface roughness changing the charge distribution on gap surfaces. In each situation plasmon coupling would behave differently depending on the localisation of field in the gap and the location and summation of all points of optical tunnelling [**barbry2015**].

To summarise, charge transfer in systems of coupled plasmons exhibit three distinct regimes of interactions. For small conductances characteristic of electron tunnelling ($1\text{–}2 \times 10^{-3}G_0$) coupling begins to be screened by the tunnelling field and the rate of redshift is steadily reduced. Upon passing through the second critical conductance at $2G_0$, also known as G_{SBDP} in the literature [**perez2010**, **perez2011**], the hybridised modes blueshift and transform into higher order CTPs due to increased screening from conductive charge flow in the gap. At this point the gap behaves as a 1D constriction subject to Landauer ballistic quantised conduction. The final conductance threshold, that for CTP excitation, has not yet been determined but instead roughly estimated to be around $30\text{–}40G_0$ from final conductance values of geometrically contacted gap surfaces. To restate the significance of this work, this is the first time these critical conductance thresholds have been measured in a dynamic dimer system through correlations between simultaneously measured optics and electronics. Using this information, the performance of a sub-nm plasmon system can begin to be characterised and quantified based upon which regime it falls under.